Progress In Electromagnetics Research B, Vol. 39, 393–409, 2012

DUAL BAND-NOTCHED UWB ANTENNA BASED ON SPIRAL ELECTROMAGNETIC-BANDGAP STRUCTURE

F. Xu, Z. X. Wang, X. Chen, and X.-A. Wang*

Key Laboratory of Integrated Microsystems, Peking University Shenzhen Graduate School, Shenzhen, Guangdong 518055, China

Abstract—An ultra-wideband (UWB) printed monopole antenna with dual band-notched characteristics is proposed. Two spiral electromagnetic-bandgap (EBG) structures placed on the front and back side of the substrate are employed to create two notch bands at 5.2 and 5.8 GHz for the lower and upper bands of the wireless local-area network (WLAN), respectively. The notch-frequency can be tuned, and the band width is narrow and adjustable. Furthermore, the spiral EBG structure used in this design are more compact than conventional mushroom-type EBG. Equivalent circuit model is extracted and discussed to explain the operating mechanism of this structure. The proposed antenna has been simulated and measured in both the frequency domain and time domain, good agreement between calculated and experimental results has been achieved.

1. INTRODUCTION

Considerable research has been done on ultra-wide band (UWB) systems, since the Federal Communications Commission (FCC) released the unlicensed frequency band of 3.1–10.6 GHz for commercial UWB applications [1]. UWB antennas are the essential part of the UWB system and have attracted more and more attentions. Printed UWB antennas are considered as promising candidates for UWB systems because of their advantages, such as low profile, light weight, and ease of fabrication [2–6].

Due to the undesired narrow band signals, such as the signal from the wireless local-area network (WLAN) (5.15–5.35 GHz, 5.725–5.825 GHz), that may interfere with the UWB systems, narrow band

Received 16 February 2012, Accepted 27 March 2012, Scheduled 4 April 2012

* Corresponding author: Xin-An Wang (anxinwang@pku.edu.cn).

interference mitigation must be considered in UWB systems design. Antennas with band-notched functions are widely used to overcome the narrow-band interference problem. The most popular strategy to provide this feature is etching a slot on the patch or ground plane [7–11] or attaching a parasitic strip to the patch or ground plane [12–16]. Complementary split ring resonator (CSRR) is also used to generate band-notched function effectively [17–20]. Multiple notched bands can be acquired by using band notched filter based on stepped impedance resonator (SIR) [21, 22]. There are even configurable UWB antennas with band notches which can be actively switched on or off by using a MEMS or a PIN diode, or tuned by means of a varactor [23–25]. Furthermore, both switchable and tunable characteristics can be achieved in the same UWB antenna by using a PIN and a varactor together [26]. However, most of these antennas have only one notch band around WLAN band. Moreover, some antennas occupy the entire 5–6 GHz frequency band which is much wider than needed (200 MHz for the lower WLAN band, 100 MHz for the upper WLAN band). Therefore, the useful spectrums are wasted and a large waveform distortion may be induced. Other antennas reject only one of the lower and upper WLAN bands.

Recently, electromagnetic-bandgap (EBG) structures coupled to the feed line have been introduced in the printed UWB antennas to generate notch bands [27–29]. In [27], four conventional mushroom-type EBG structures with size of $8.5 \times 8.5\,\text{mm}^2$ are used to generate a notch band of 0.7 GHz around 5.5 GHz. However, The EBG structures occupy too much area and the single notch band of 0.7 GHz is wider than needed, therefore the spectrum between 5.35 to 5.725 GHz is wasted. In [28], two edge-located vias mushroom-type EBG (ELV-EBG) placed at different sides of the microstrip feed line are utilized to create two notch bands for the 5.2 and 5.8 GHz WLAN bands, respectively. Owing to the notch-band width controllable capacity and the attenuation of the coupling between notch designs, high efficient band-notched functions are achieved. However, the reflection value at resonant frequency decreased along with the reduction of the bandwidth, so there is a trade-off between the reflection value and the bandwidth. In addition, the ELV-EBG structure adopted in [28] instead of conventional mushroom-type EBG doesn't reduce the size significantly.

In this paper, a printed monopole UWB antenna with two sharp notch bands for lower and upper WLAN band respectively is presented. Two spiral EBG structures are employed to obtain the dual band-notched functions. One of these structures is on the front side coupled to the feed line; the other is on the back side coupled to the ground

plane, thus the coupling between them can be weakened effectively. The resonant frequency and bandwidth of the notch band can be controlled by tuning the parameters of the spiral EBG structure. Furthermore, by increasing the inductance of the resonant circuit, this structure is much more compact than conventional mushroom-type EBG. This paper is organized as follows. In Section 2, a parameter study of the spiral EBG structure is performed to analyze the effect of physical parameters on the band-notched characteristic and size of the EBG structure. In Section 3, a dual band-notched UWB antenna based on spiral EBG structures is designed. Besides, simulated and measured results in both frequency and time domain for this antenna are also shown in this section.

2. PARAMETER STUDY OF SPIRAL EBG STRUCTURE

Spiral EBG structures have been studied in [30, 31], which are used for multi-chip module packages noise isolation and high-speed circuits wideband ground bounce noise suppression, respectively. In this section, a spiral EBG composed of a spiral-shaped strip and a via hole is utilized to generate a narrow notch band.

A microstrip line based approach suggested in [28] is adopted to study the band-notched characteristic. As shown in Figure 1(a), a spiral EBG structure is located in the vicinity of the microstrip feed line with a gap g. The width of the spiral strip is W, the gap is s, the radius of the via hole is r and the number of turns is N. A lossless substrate with thickness of 0.762 mm and relative permittivity of 3.66 is used for calculation. The 50-Ω microstrip feed line is of 1.67 mm width. As shown in Figure 1(b), an equivalent circuit model based on LC resonator is derived to explain the operating mechanism of the spiral EBG structure coupled to the microstrip feed line. In this model, C_s denotes the capacitance between the EBG and the ground plane. The capacitance C_h is used to represent the coupling between the EBG and the microstrip feed line. L_v is due to the current flowing through the via. The inductance L_h is generated by the current flowing through the spiral structure. Therefore, the resonant frequency is given by:

$$f_r = 1/2\pi\sqrt{(L_v + L_h)(C_s + C_h)}. \quad (1)$$

As indicated in (1), L_h increases the total lumped inductance of the EBG structure, thus for the same resonant frequency, smaller capacitance C_s is needed. Since C_s is proportional to the area of EBG structure, compact dimension can be achieved.

As shown in Figure 1(c), three EBGs with $N = 0$, 1, 2 ($N = 0$ corresponds to conventional mushroom-type EBG) and different W

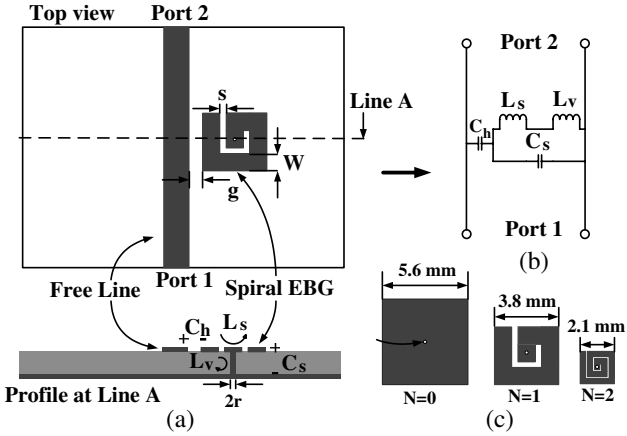

Figure 1. (a) Schematic of microstrip line based approach. (b) Equivalent circuit model. (c) EBG structures with $N = 0$, 1, 2.

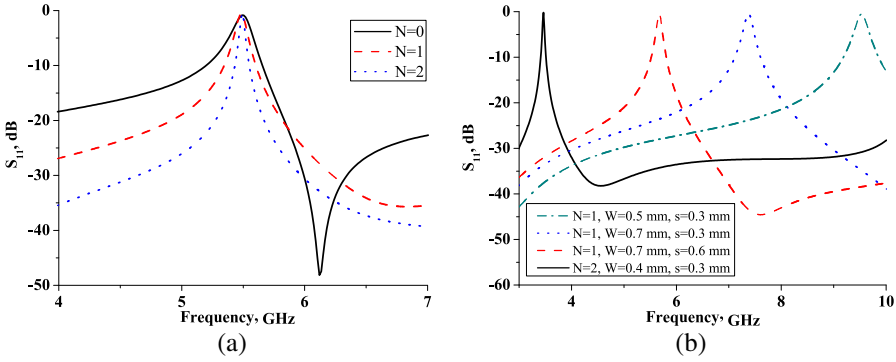

Figure 2. (a) Effect of the number of turns N on the width of the notch band. (b) Effect of W, s and N on the resonant frequency.

and s are employed to investigate the effect of parameters on the bandwidth of the notch band. It is clearly seen from Figure 2(a) that the the three EBGs have almost same resonant frequency and reflection value, while N changes from 0 to 2, the bandwidth decreases from 470 to 100 MHz. The geometric dimensions and band-notched characteristics of the three EBGs are listed in Table 1. We can see that compared to conventional EBG structure, the size of spiral EBG with $N = 2$ is significantly reduced by 86%, and a sharp notch band of 100 MHz is achieved, which can be used to filter the narrow band interference accurately and decrease the waveform distortion effectively.

Table 1. Various spiral EBGs for parameter study.

N	W (mm)	s (mm)	f_r (GHz)	Bandwidth (MHz)	Size (mm^2)	Size Reduction (%)
0	–	–	5.5	470	5.6×5.6	0
1	1.1	0.15	5.5	250	3.8×3.8	54
2	0.3	0.15	5.5	100	2.1×2.1	86
1	0.5	0.3	9.5	680	2.1×2.1	–
1	0.7	0.3	7.4	500	2.7×2.7	–
1	0.7	0.6	5.7	300	3.3×3.3	–
2	0.5	0.3	3.5	100	3.7×3.7	–

Figure 2(b) presents the effect of W, s and N on the resonant frequency. When W is increased from 0.5 to 0.7 mm, s is fixed at 0.3 mm, N is fixed at 1, the notch frequency is decreased from 9.5 to 7.4 GHz. When s is increased from 0.3 to 0.6 mm, W is fixed at 0.7 mm, N is fixed at 1, the notch frequency is decreased from 7.4 to 5.7 GHz. When N is increased from 1 to 2, W is fixed at 0.5 mm, s is fixed at 0.3 mm, the notch frequency is decreased significantly from 9.5 to 3.5 GHz. Therefore, the notch frequency can be tuned though the whole UWB band from 3.1 to 10.6 GHz by changing the parameters W, s and N. Furthermore, the parameter N can be used to coarse tune the resonant frequencies in a wide range, while the parameters W and s can be used to fine tune the notch frequency in a narrow range. Relevant parameters of EBGs with different resonant frequency are also summarized in Table 1.

3. DUAL BAND-NOTCHED UWB ANTENNA

3.1. Antenna Design

The proposed antenna is illustrated in Figure 3. It consists of a staircase rectangular patch on the front side and a ground plane with an open slot on the back side to obtain optimum impedance matching. The antenna is fabricated on a high-frequency substrate Ro4350B ($\varepsilon_r = 3.66$) of $30 \times 35\,mm^2$ dimension, 0.762 mm thickness and 0.5 oz electrodeposited copper. A 50-Ω microstrip feed line with width of 1.67 mm is used to feed the path. Figure 4 presents the photograph of the fabricated antenna. A SMA connector is mounted on the edge to connect the antenna to a vector network analyzer for measurement. To generate dual narrow notch bands, two spiral EBG structures are employed. One of these two structures (EBG1)

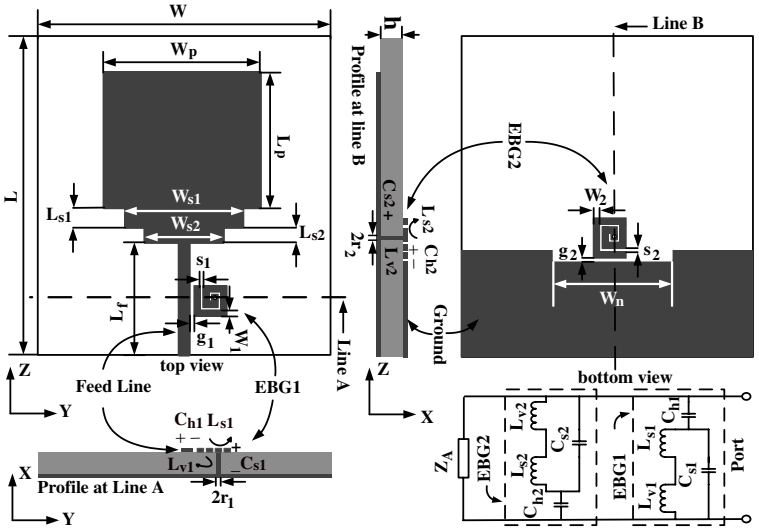

Figure 3. Geometry of the proposed antenna.

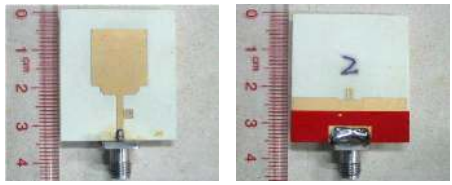

Figure 4. Photograph of the fabricated antenna. (a) Top view. (b) Bottom view.

coupled to the microstrip feed line is located on the front side of antenna to reject interference from the upper WLAN band; the other (EBG2) coupled to the ground plane is placed on the back side to filter noise from the lower WLAN band. Since these two structures are separated from each other and fabricated on different sides, the coupling between them can be attenuated effectively. The spiral EBG structure employed in this design with resonant frequency at WLAN band is of size around $2.5 \times 2.5\,\text{mm}^2$ which is more compact than ELV-EBG structure resonating at the same frequency of about $4.9 \times 4.9\,\text{mm}^2$ dimension [28]. The antenna parameters are shown in Table 2. A reference antenna without EBG structures are also fabricated and measured for comparison.

As shown in Figure 3, an equivalent circuit model is extracted to describe the operating mechanism of this dual band-notched UWB

Table 2. Parameters of the fabricated antenna (Unite:mm).

W	L	L_f	W_{s1}	L_{s1}	W_{s2}	L_{s2}	W_p	L_p	h
30	35	12	10.5	1.5	9	1	15	14.5	0.762
W_1	s_1	N_1	g_1	r_1	W_2	s_2	N_2	g_2	r_2
0.47	0.2	1.5	0.2	0.1	0.42	0.2	1.75	0.15	0.1

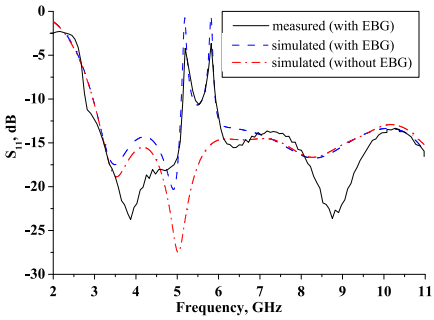

Figure 5. Simulated and measured return loss of the proposed dual band-notched antenna.

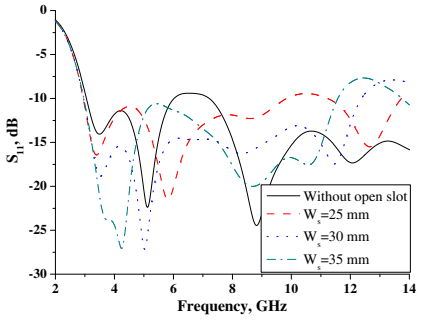

Figure 6. Simulated return loss of the reference antenna with various W and of the reference antenna without the open slot.

antenna with two spiral EBG structures. Therefore, the notch frequencies can be calculated by:

$$f_{r1} = 1/2\pi\sqrt{(L_{v1} + L_{h1})(C_{s1} + C_{h1})}. \quad (2)$$

$$f_{r2} = 1/2\pi\sqrt{(L_{v2} + L_{h2})(C_{s2} + C_{h2})}. \quad (3)$$

3.2. Results and Discussions

The proposed dual band-notched UWB antenna was designed and optimized with CST microwave studio and measured by an Agilent N5230A vector network analyzer. Figure 5 shows the simulated and measured return loss (S_{11}) of the proposed antenna. Furthermore, the simulated result of the reference antenna without spiral EBG structure is also displayed for comparison. As shown in Figure 5, the proposed antenna has two sharp notch bands of 5.16–5.47 GHz and 5.62–5.97 GHz, and exhibits excellent wideband performance. Good agreement between simulation and measurement is achieved.

For this kind of small antennas, not only the radiating element but also the ground plane contributes to the radiation. Therefore a parameter study of the reference antenna ground plane is performed

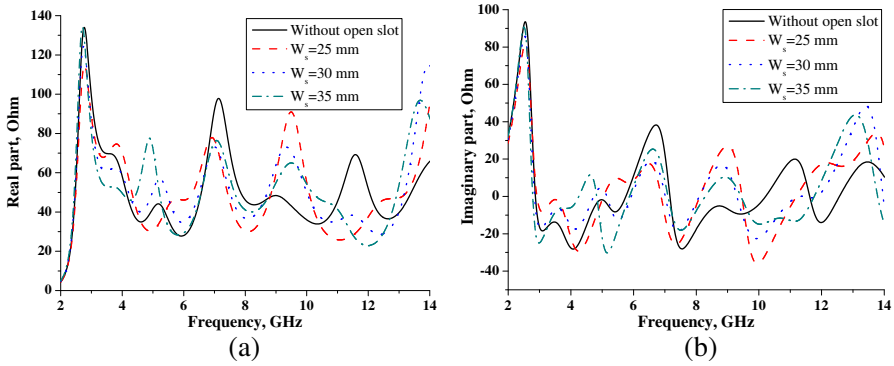

Figure 7. Simulated input impedance of the reference antenna with various W and of the reference antenna without the open slot.

to examine the effect of its size and the open slot on the bandwidth and the input impedance. Figure 6 presents the simulated return loss curves for the reference antenna with various ground plane widths (W) and for the reference antenna without the open slot when W is fixed at 30 mm. It can be observed that the -10 dB bandwidth is heavily dependent on the width W. The optimized ground plane width adopted by the proposed antenna is 30 mm. Furthermore, the performance of the antenna from 6 to 8 GHz is greatly improved by inserting and open slot into the ground plane, as shown in Figure 6. The simulated real part and imaginary part of the reference antenna input impedance are plotted in Figures 7(a) and (b), respectively. It can be seen that the ground plane width W also significantly influences the input impedance of the antenna and the best impedance matched to 50-Ω is achieved at $W = 30$ mm. Also the impedance of the reference antenna from 6 to 8 GHz is pulled close to 50-Ω by embedding an open slot into the ground plane, which results in better impedance matching in this band.

To verify the weak coupling between the two spiral EBG structures with similar resonant frequency, a parameter study is made. Simulated return loss of proposed antenna for various W_1 is exhibited in Figure 8(a). It shows that the upper notch frequency increases from 5.82 to 6.96 GHz as W_1 decreases from 0.47 to 0.37 mm, while the lower notch frequency is almost unchanged for different W_1. The return loss of proposed antenna for various W_2 is plotted in Figure 8(b). The lower notch frequency decreases from 5.21 to 4.37 GHz by tuning W_2 from 0.42 up to 0.52 mm, while the upper notch frequency is invariable during the process. Therefore, owing to the week coupling between

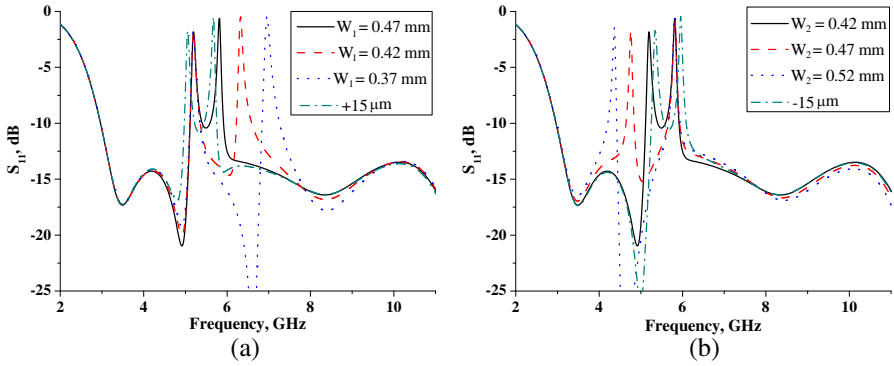

Figure 8. (a) Simulated return loss for the proposed antenna with different W_1. (b) Simulated return loss for the proposed antenna with different W_2.

the two spiral EBGs, efficient dual band-notched characteristics are obtained. Moreover, to analyze the sensitivity of the proposed dual band-notched antenna affected by the fabrication tolerances in practice, a simulation is performed. In this simulation, the variation value of W_1 and W_2 is set to $\pm 15\,\mu$m, which is the track width tolerance for 0.5 oz copper announced by the manufacturer. As shown in Figures 8(a) and (b), the two notched bands are slightly sensitive to the widths of the EBG structures, the corresponding shift is about 150 MHz.

For further understanding the operational mechanism of the proposed antenna with dual band-notched functions, current distributions at 4, 5.2, 5.8 and 8 GHz are simulated and illustrated in Figures 9(a), (b), (c) and (d), respectively. It can be observed from Figures 9(a) and (d) that the current distribution on EBGs are weak at 4 and 8 GHz. It implies that the EBG structures have little effect on the antenna at pass band. As shown in Figure 9(b), the current distribution of 5.2 GHz is mainly concentrated on the EBG2, while the current on radiating patch and EBG1 are weak. Figure 9(c) shows that the current distribution of 5.8 GHz is large on EBG1 and week on radiating patch and EBG2. It indicates that the two EBGs operate as resonators and reflect the current to prevent the antenna from radiating. Furthermore, these two EBGs have week effect on each other, which is also demonstrate in Figure 8.

The simulated and measured radiation patterns at 4 and 8 GHz are illustrated in Figure 10. The antenna presents a stable quasi-omnidirectional pattern in XY-plane. As indicated in Figure 11, the

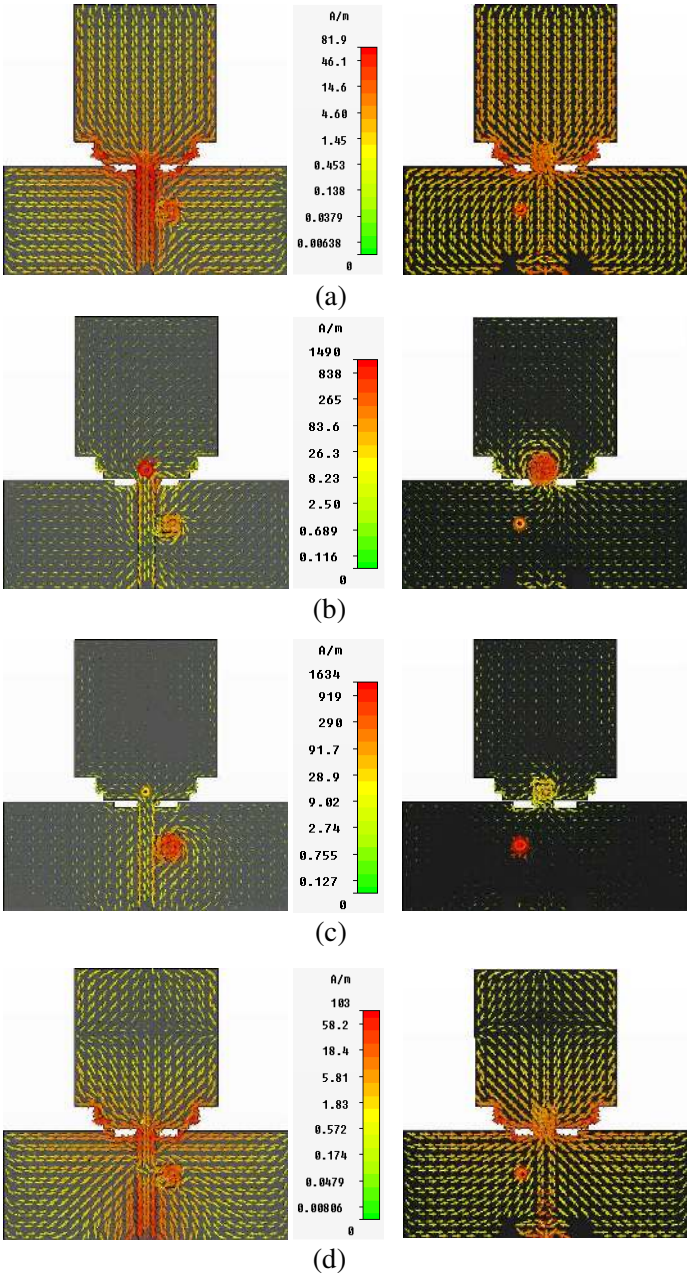

Figure 9. Current distributions of the proposed antenna (left: top view, right: bottom view) at (a) 4 GHz, (b) 5.2 GHz, (c) 5.8 GHz and (d) 8 GHz.

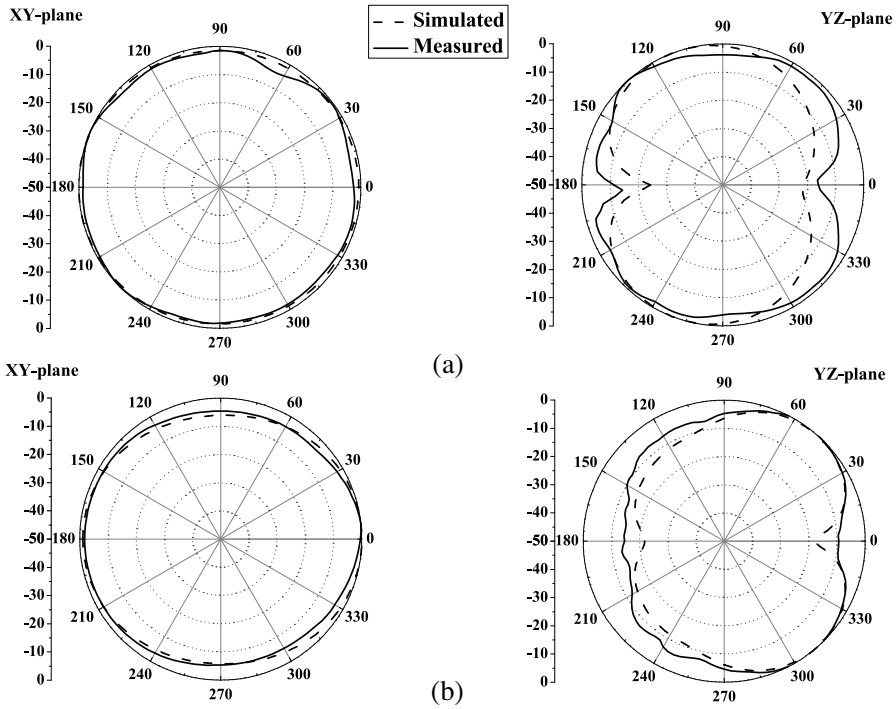

Figure 10. Measured radiation pattern of the proposed antenna in XY- and YZ-plane at (a) 4 GHz and (b) 8 GHz.

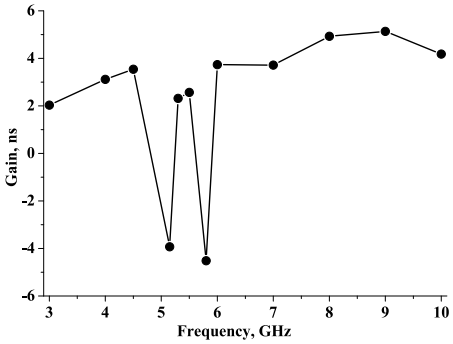

Figure 11. Gain of the proposed antenna.

gain of proposed antenna drops steeply in the lower and upper WLAN band. A gain suppression around 7 dB is achieved in this design. Figure 12 presents the measured transfer function (S_{21}) and group

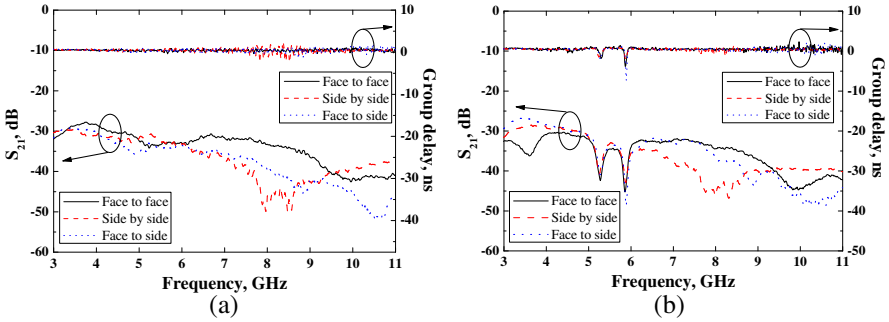

Figure 12. Measured transfer function and group delay for (a) the reference antenna and (b) the proposed antenna.

delay of the reference and proposed antenna. two identical proposed antennas face to face with a distance of 200 mm. A pair of identical proposed antennas with dual notched bands was mounted on the two ports of the Agilent N5230A network analyzer with a distance of 200 mm indoor. The proposed antennas served as transmitting and receiving antennas, respectively. Three typical orientations including face to face, side by side and face to side were considered in the measurement. In order to obtain accurate experimental results, the reference planes were calibrated to the antenna terminals by using an Agilent N4433A electronic calibration module, and the transmitting power was set to 0 dBm. The measurement was also performed using a pair of reference antennas in the same way. It can be seen from Figure 12(a) that the transfer function curves for the reference antenna keep smooth over the entire UWB band. However, in the side by side condition, the transfer function drops at frequencies higher than 8 GHz and a fluctuation of the group delay is also observed. This can be explained by the decrease of radiation pattern in Y-Direction, as shown in Figure 10(b). Figure 12(b) shows that two sharp notches of the transfer function occur at 5.2 and 5.8 GHz for all the three orientations. Due to the resonant behavior of the spiral EBG structures, dramatic variations of the group delay in the two notched bands are also found.

To examine the antenna performance in time domain, the distortion and dispersion of a test pulse are analyzed in detail. The test pulse is used to excited the UWB antenna as an input signal, which is given by

$$u(t) = \cos(2\pi f_c t) \exp\left[-2\pi (t/\tau)^2\right]. \tag{4}$$

where the f_c and τ are set to the same value as in [32]. The spectrum of the output pulse in frequency domain is the product of

the measured transfer function and the spectrum of input pulse. Then the output pulse in time domain can be calculated by using inverse Fourier transform. The normalized input and output pulses of the reference and proposed antennas for the three orientations are shown in Figures 13(a) and (b), respectively. The output pulses are shifted backward in time to eliminate the overlap with input pulse due to the small separation (200 mm) between the transmitting and receiving antennas. In this design, two figures of merit are adopted to qualify the pulse distortion and dispersion. One is the fidelity factor (F) [33], which is used to evaluate the degree of similarity between the input and output pulses. It is defined as

$$F = \max_{\tau} \left[\frac{\int_{-\infty}^{\infty} s_t(t) s_r(t+\tau) dt}{\sqrt{\int_{-\infty}^{\infty} s_t^2(t) dt \int_{-\infty}^{\infty} s_r^2(t) dt}} \right]. \tag{5}$$

where $s\,(t)$ and $r\,(t)$ are the input and output signals, respectively. The other is the output-to-input ratio of the time window containing 90% of the pulse energy (RE90) [34]. This figure of merit is introduced to evaluate the dispersion of output pulse caused by ringing effect. For the measured output pulses shown in Figure 13, the calculated fidelity factors and RE90 of them are listed in Tables 3 and 4, respectively.

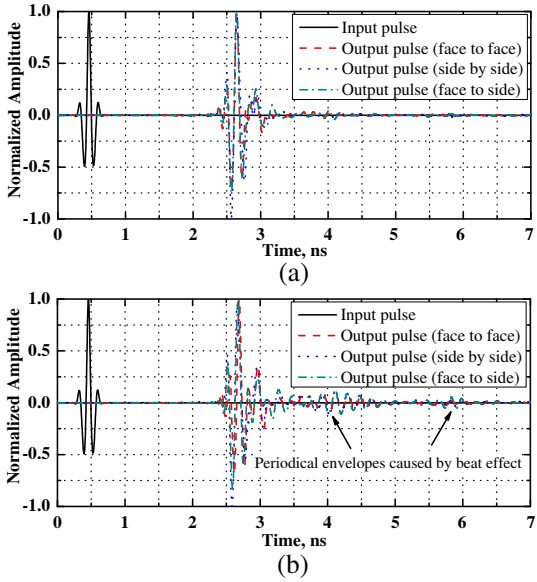

Figure 13. Shifted and normalized input and output pulse in time domain for (a) the reference antenna and (b) the proposed antenna.

Table 3. Measured fidelity factor and E90 for the reference antenna.

	Face to Face	Side by Side	Face to Side
Fidelity Factor (%)	93.6	79.3	88.4
E90	1.29	1.61	1.55

Table 4. Measured fidelity factor and E90 for the proposed antenna.

	Face to Face	Side by Side	Face to Side
Fidelity Factor (%)	89.7	81.4	86.4
E90	2.63	2.84	2.76

It is worth noting that the RE90 of proposed antenna is more than 2, which means that the dispersions of output pulses are relative large. This phenomenon can be explained by the beat effect which arises from the fact that the two EBG structures have similar resonant frequencies. Due to this effect, the output pulse amplitude after the peak is not a monotone decreasing function of time and some periodical envelopes are observed in Figure 13(b).

4. CONCLUSION

A novel UWB printed antenna with dual narrow band-notched behavior for the lower and upper WLAN bands has been realized and discussed in detail. The dual notched bands were created by using two compact spiral EBG structures on the front side coupled to the feed line and on the back side coupled to the ground plane, respectively. An equivalent circuit model of propose antenna with two spiral EBGs was built and analyzed. Good agreement between simulated and measured results was achieved. This proposed antenna is expected to be an excellent candidate for UWB applications in complex electromagnetic environment, due to its effective dual band-notched function based on compact spiral EBG structure.

REFERENCES

1. First Report and Order, "Revision of part 15 of the commission's rule regarding ultra-wideband transmission system FCC02-48," Federal Communications Commission, 2002.

2. Liang, J., C. C. Chiau, X. Chen, and C. G. Parini, "Printed circular disc monopole antenna for ultra wideband applications," *Electronics Letters*, Vol. 40, No. 20, 1246–1248, 2004.
3. Choi, S. H., J. K. Park, S. K. Kim, and J. Y. Park, "A new ultra-wideband antenna for UWB applications," *Microwave and Optical Technology Letters*, Vol. 40, No. 5, 399–401, 2004.
4. Lin, C. C., Y. C. Kuo, and H. R. Chuang, "A planar triangular monopole antenna for UWB communication," *IEEE Microwave and Wireless Components Letters*, Vol. 15, No. 10, 624–626, 2005.
5. Xu, H.-Y., H. Zhang, K. Lu, and X.-F. Zeng, "A holly-leaf-shaped monopole antenna with low RCS for UWB application," *Progress In Electromagnetics Research*, Vol. 117, 35–50, 2011.
6. Lin, S., R.-N. Cai, G.-L. Huang, and J.-X. Wang, "A miniature UWB semi-circle monopole printed antenna," *Progress In Electromagnetics Research Letters*, Vol. 23, 157–163, 2011.
7. Su, S. W., K. L. Wong, and C. L. Tang, "Band-notched ultra-wideband planar monopole antenna," *Microwave and Optical Technology Letters*, Vol. 44, No. 3, 217–219, 2005.
8. Cho, Y. J., K. H. Kim, D. H. Choi, S. S. Lee, and S.-O. Park, "A miniature UWB planar monopole antenna with 5-GHz band-rejection filter and the time-domain characteristics," *IEEE Transactions on Antennas and Propagation*, Vol. 54, No. 5, 1453–1460, 2006.
9. Li, W.-M., T. Ni, S.-M. Zhang, J. Huang, and Y.-C. Jiao, "UWB printed slot antenna with dual band-notched characteristic," *Progress In Electromagnetics Research Letters*, Vol. 25, 143–151, 2011.
10. Fan, S.-T., Y.-Z. Yin, H. Li, and L. Kang, "A novel self-similar antenna for UWB applications with band-notched characteristics," *Progress In Electromagnetics Research Letters*, Vol. 22, 1–8, 2011.
11. Dong, Y. D., W. Hong, Z. Q. Kuai, and J. X. Chen, "Analysis of planar ultrawideband antennas with on ground slot band notched structures," *IEEE Transactions on Antennas and Propagation*, Vol. 57, 1886–1893, 2009.
12. Zhang, G.-M., J.-S. Hong, and B.-Z. Wang, "Two novel band-notched UWB slot antennas fed by microstrip line," *Progress In Electromagnetics Research*, Vol. 78, 209–218, 2008.
13. Mardani, H., C. Ghobadi, and J. Nourinia, "A simple compact monopole antenna with variable single- and double-filtering function for uwb applications," *IEEE Antennas and Wireless*

Propagation Letters, Vol. 9, 1076–1079, 2010.

14. Yazdi, M. and N. Komjani, "A compact band-notched UWB planar monopole antenna with parasitic elements," *Progress In Electromagnetics Research Letters*, Vol. 24, 129–138, 2011.
15. Ryu, K. S. and A. A. Kishk, "UWB antenna with single or dual band-notches for lower WLAN band and upper WLAN band," *IEEE Transactions on Antennas and Propagation*, Vol. 57, No. 12, 3942–3950, 2009.
16. Chen, H., Y. Ding, and D. S. Cai, "A CPW-FED UWB antenna with WIMAX/WLAN band-notched characteristics," *Progress In Electromagnetics Research Letters*, Vol. 25, 163–173, 2011.
17. Kim, D. O., N.-I. Jo, H.-A. Jang, and C.-Y. Kim, "Design of the ultrawideband antenna with a quadruple-band rejection characteristics using a combination of the complementary split ring resonators," *Progress In Electromagnetics Research*, Vol. 112, 93–107, 2011.
18. Kim, J., C. S. Cho, and J. W. Lee, "5.2 GHz notched ultra-wideband antenna using slot-type SRR," *Electronics Letters*, Vol. 42, No. 6, 315–316, 2006.
19. Tang, M.-C., S. Xiao, T. Deng, D. Wang, J. Guan, B. Wang, and G.-D. Ge, "Compact UWB antenna with multiple band-notches for WiMAX and WLAN," *IEEE Transactions on Antennas and Propagation*, Vol. 59, No. 4, 1372–1396, 2011.
20. Lai, H., Z.-Y. Lei, Y.-J. Xie, G.-L. Ning, and K. Yang, "UWB antenna with dual band rejection for WLAN/wimax bands using csrrs," *Progress In Electromagnetics Research Letters*, Vol. 26, 67–78, 2011.
21. Zhang, Y., W. Hong, C. Yu, J.-Y. Zhou, and Z.-Q. Kuai, "Design and implementation of planar ultra-wideband antennas with multiple notched bands based on stepped impedance resonators," *IET Microwave, Antennas and Propagation*, Vol. 3, No. 7, 1051–1059, 2009.
22. Zhang, Y., W. Hong, Z. Q. Kuai, and J. Y. Zhou, "A compact multiple bands notched UWB antenna by loading SIR and SRR on the feed line," *Proc. ICMMT*, Vol. 1, No. 7, 198–201, 2008.
23. Nikolaou, S., N. D. Kingsley, G. E. Ponchak, J. Papapolymerou, and M. M. Tentzeris, "UWB elliptical monopoles with a reconfigurable band notch using MEMS switches actuated without bias lines," *IEEE Transactions on Antennas and Propagation*, Vol. 57, No. 8, 2242–2251, 2009.
24. Sim, C.-Y.-D., W.-T. Chung, and C.-H. Lee, "Planar UWB

antenna with 5 GHz band rejection switching function at ground plane," *Progress In Electromagnetics Research*, Vol. 106, 321–333, 2009.

25. Antonino-Daviu, E., M. Cabedo-Fabres, M. Ferrando-Bataller, and A. Vila-Jimenez, "Active UWB antenna with tunable band-notched behaviour," *Electronics Letters*, Vol. 43, No. 18, 959–960, 2007.
26. Xu, F., L. Tang, X. Chen, and X.-A. Wang, "Active UWB printed antenna with tuanble and switchable band-notched functions," *Progress In Electromagnetics Research Letters*, Vol. 30, 21–28, 2012.
27. Yazdi, M. and N. Komjani, "Design of a band-notched UWB monopole antenna by means of an EBG structure," *IEEE Antennas and Wireless Propagation Letters*, Vol. 10, 170–173, 2011.
28. Peng, L. and C.-L. Ruan, "UWB band-notched monopole antenna design using electromagnetic-bandgap structures," *IEEE Transactions on Antennas and Propagation*, Vol. 59, No. 4, 1074–1081, 2011.
29. Ren, F.-C., F.-S. Zhang, J. H. Bao, Y.-C. Jiao, and L. Zhou, "Printed bluetooth and UWB antenna with dual band-notched functions," *Progress In Electromagnetics Research Letters*, Vol. 26, 39–48, 2011.
30. Kamgaing, T. and O. M. Ramahi, "Multiband electromagnetic-bandgap structures for applications in small form-factor multichip module packages," *IEEE Transactions on Microwave Theory and Techniques*, Vol. 56, No. 10, 2293–2300, 2008.
31. Wang, C.-L., G.-H. Shiue, W.-D. Guo, and R.-B. Wu, "A systematic design to suppress wideband ground bounce noise in high-speed circuits by electromagnetic-bandgap-enhanced split powers," *IEEE Transactions on Microwave Theory and Techniques*, Vol. 54, No. 12, 4209–4217, 2006.
32. Costa, J., C. Medeiros, and C. Fernandes, "Performance of a crossed exponentially tapered slot antenna for UWB systems," *IEEE Transactions on Antennas and Propagation*, Vol. 57, No. 5, 1345–1352, 2011.
33. Klemm, M. and G. Troster, "Characterization of small planar antennas for UWB mobile terminals," *Wireless Communications and Mobile Computing*, Vol. 5, No. 5, 525–536, 2005.
34. Medeiros, C., J. Costa, and C. Fernandes, "Compact tapered slot UWB antenna with WLAN band rejection," *IEEE Antenna and Wireless Propagation Letters*, Vol. 8, 661–664, 2009.